



# Biogenic Synthesis of Novel Ag-Ni Bimetallic Nanoparticles : Characterization and Photocatalytic Activity on Malachite Green

Anuradha Ch.S.<sup>1</sup>, Prof. Susheela Bai G.<sup>2</sup>, Dr. Kishore Babu B<sup>3</sup>.

Dr.Tanseem Mohammed<sup>4</sup>

<sup>1,2,3</sup> Department of Engineering Chemistry, AUCE (A), Andhra University,  
Visakhapatnam, Andhra Pradesh, India.

<sup>4</sup> Associate Professor, Chemistry Division, Ibn Sina National College for  
Medical Sciences, Jeddah , Saudi Arabia

## ABSTRACT

An environmentally benign cost effective method was reported for green synthesis of Ag-Ni bimetallic nanoparticles by using *Aerva Lanata* leaf extract. The phyto molecules present in the extract are acting as reducing agents, stabilizing and capping agents for the biosynthesized nano particles. The characterization studies were done by UV-VIS , FTIR spectroscopies , SEM, XRD, EDX and HRTEM analyses. These nanoparticles were further applied as photocatalysts for degradation of Malachite Green dye by irradiation under sunlight. From this present study on bimetallic Ag-Ni nanoparticles synthesized from *Aerva lanata* leaf extract, the optimum conditions found in the degradation of malachite green dye is pH 8, weight of catalyst 30 mg, dye concentration of 10 ppm and contact time of 120 minutes. A maximum photodegradation of ~ 85-89% could be obtained under these optimum conditions.

## KEY WORDS

Bimetallic nanoparticles (BMNPs), *Aerva Lanata*(AL), Malachite Green (MG), photo degradation.

## INTRODUCTION

Nanotechnology involves the synthesis and application of materials having one of the dimensions in the range of 0.1-100 nm and acts as a channel between bulk materials and atomic or molecular structures.[1] In recent times bimetallic nanoparticles have gained considerable attention because of their importance for magnetic, optical and catalytic applications in multiple fields[2],[3]. Various physical, chemical and biological methods have been employed for the synthesis of bimetallic nanoparticles[4][5]. Several advantages of biological methods over physical and chemical methods are the biological process is environmentally benign, less time consuming, cost effective with almost negligible industrial waste without use of toxic chemicals[6]. Biosynthesized bimetallic nanoparticles are used in several contemporary fields viz. imaging, labeling, luminescence tagging, drug delivery and biomedical field because of their superior properties. Biosynthesized bimetallic nanoparticles additionally have been found to possess extraordinary catalytic activities[7].

Dyes are used widely in various fields such as cosmetics, leather, food and textile industries. The release of these industrial dye effluents into water shows adverse effect on quality of water[8]. One of such dye is malachite green (MG).

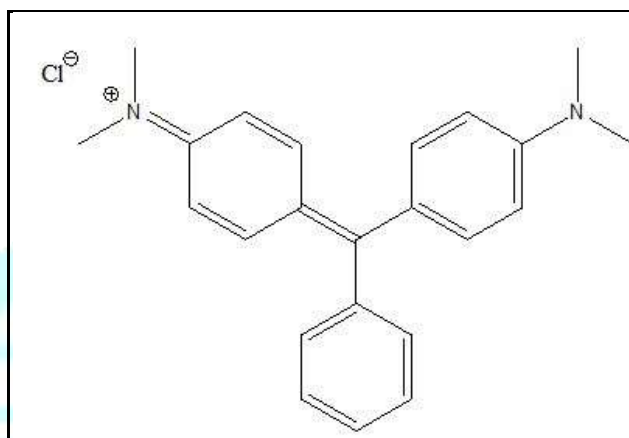


Figure 1 (a) : Structure of Malachite Green dye

Malachite green dye is a cationic green crystalline water soluble dye and belongs to triphenylmethane category[9]. (Figure 1.a). MG dye is a potential environmental contaminant and a peril to public health as it is a multi-organ toxin proved as by both experimental clinical observations [10]. So it is necessary to exterminate the MG dye effluents from water. Many chemical, physical and biological treatment methods including adsorption, precipitation filtration, electro dialysis, coagulation, oxidation and membrane separation are used in the treatment of dye effluents[11]. Dye removal via degradation using photocatalysts is the most scatheless and desirable among all methods because of its sustainable and ecofriendly technology[12][13]. Recent times nanotechnology has been extended in the waste water treatment and nanoparticles are used as photocatalysts for degradation of dyes due to their extensive surface area[14].

Herein, an effortless and robust green method for synthesis of Ag-Ni bimetallic nanoparticles (BMNPs) by using leaf extract of *Aerva lanata* as a stabilizing, reducing and capping agent was reported and by using these BMNPs as catalysts for photodegradation of MG dye carried under solar light irradiation was also studied at various reaction conditions to observe the optimum conditions for the maximum photodegradation.

## 2. EXPERIMENTAL

**2.1. Materials:** Chemical reagents used (silver nitrate and nickel nitrate) in this study were of analytical grade. Deionised water was used to clean glassware, to prepare chemical solutions and for experimental procedure. Fresh leaves of *Aerva lanata* were collected from agricultural fields in S.Kota, Vizianagaram district, Andhra Pradesh state, India.

**2.2. Preparation of *Aerva lanata* leaf extract:** 100g of fresh leaves were weighed and thoroughly washed with running tap water to remove detritus on surface of leaves followed by deionised water to get rid of other contaminants from leaves and dried up under shade for 10 days. These leaves were cut into tiny pieces and made homogenized powder by using home blender. The procured powder placed in refrigerator at

4°C which was kept in an air tight container. Now 200 mL deionised water was taken in 500 mL beaker to this 10g stored powder was weighed and added. The contents in the beaker heated for 30 minutes at 50°C with occasional stirring with glass rod and then cooled to acquire room temperature. The cooled concoction was filtered 2 times with Whatman No.1 filter paper and reserved in refrigerator at 4°C. This was taken as leaf extract throughout the experiment (Figure : 1.(b)1(c)).



Figure 1(b): *Aerva Lanata* plant



Figure 1(c): *Aerva Lanata* leaf extract

### 2.3. Synthesis of Ag-Ni bimetallic nanoparticles:

Equimolar (25 mM) concentrations of silver nitrate and nickel nitrate aqueous solutions were prepared separately in 100 ml volumetric flasks by dissolving 0.4246 g, 0.7267 g weight of  $\text{AgNO}_3$  and  $\text{Ni}(\text{NO}_3)_2$  in deionized water respectively. Synthesis of Ag-Ni BMNPs was done by taking 100mL of  $\text{AgNO}_3$  solution in a 500 mL beaker, to this 90ml of leaf extract, 100mL of  $\text{Ni}(\text{NO}_3)_2$  solution were added by drop wise in simultaneous addition process. After this addition the beaker was placed on a magnetic stirrer for continuous agitation. This mixture was stirred at 70°C for 60 minutes at pH 8 on magnetic stirrer. These synthesized BMNPs were separated out by doing centrifugation at 5000 rpm for 40 minutes. The obtained BMNPs were washed with deionised water 2 times to remove unwanted constituents and dried in oven at 80°C for two hours. The resultant BMNPs particles were collected (figure: 1(d)) and used for characterization.



Figure : 1(d) . Synthesis of Ag-Ni BMNPs from precursor solutions

## 2.4. Characterization:

Formation of Ag-Ni BMNPs was confirmed by UV-Visible absorption spectra using UV-2450 SHIMADZU double beam spectrophotometer, FTIR using Bruker, SEM, EDX studies are done by using Hitachi S-3700N machine and the morphology of BMNPs was elucidated by HRTEM analysis with FEI Technai machine.

## 3. RESULTS AND DISCUSSION

### 3.1. UV-Visible spectral analysis:

UV-Visible spectrum of *Aerva Lanata* leaf extract is given in Figure 2(a). UV-Visible absorption spectrum of Ag-Ni BMNPs is presented in Figure 2(b). The characteristic surface plasmon resonance (SPR) band at around 438 nm is observed in Ag-Ni BMNPs which confirms the nano size of the synthesized BMNPs[15].

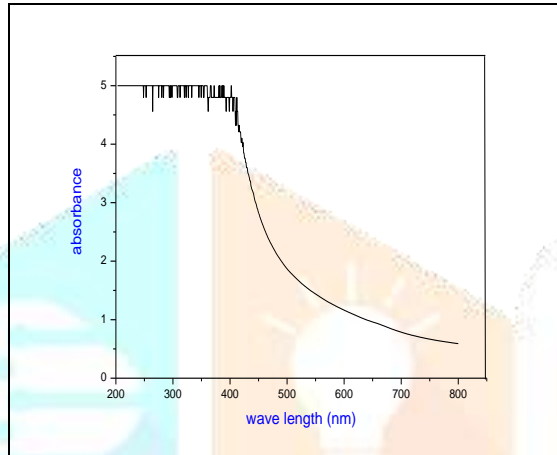


**Figure 2 (a):** UV-VIS Spectrum of *Aerva Lanata* leaf extract

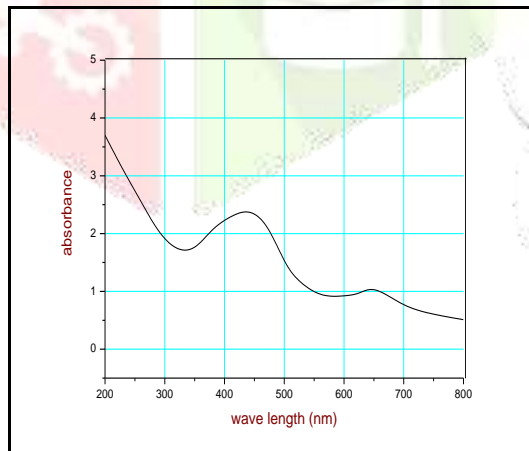


**Figure.2(b):** UV-Visible absorption spectrum of Ag-Ni BMNPs

### 3.2. FTIR spectral analysis:

FTIR spectral data is used to identify different functional groups present in biomolecules of leaf extract. These groups are responsible for the bioreduction of  $\text{Ag}^+$ ,  $\text{Ni}^{+2}$  precursors and also for capping and stabilization of Ag-Ni BMNPs. The intense peaks were observed and compared with standard values to analyze the functional groups in *Aerva lanata* leaf extract and greensynthesized Ag-Ni BMNPs. FTIR spectra of *Aerva lanata* leaf extract and synthesized Ag-Ni BMNPs by using *Aerva lanata* leaf extract were shown in **Figure.3 (a)** and **Figure.3 (b)** respectively. The comparison of the FTIR spectra of both Ag-Ni BMNPs and leaf extract of *Aerva lanata* clearly indicates the existence of

the plant extract phytomolecules such as polyphenols, terpenes, flavonoids, glycosides, tannins, sterols, amides, carbohydrates, amines the surface of the Ag-Ni BMNPs [16,17].

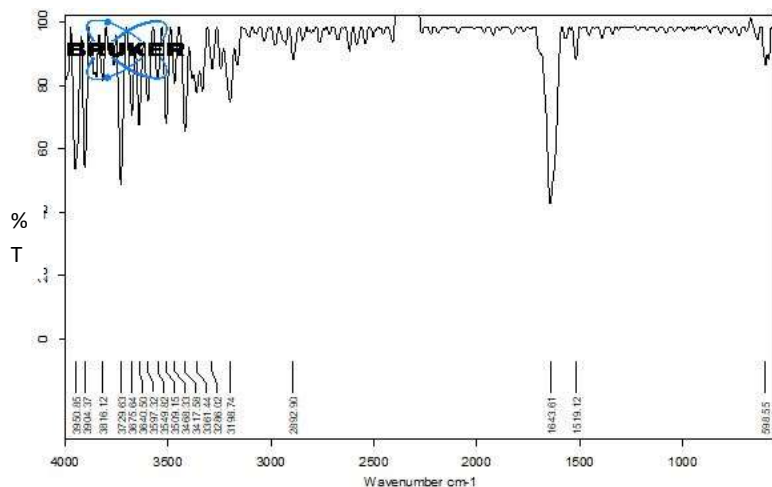


Figure.3 (a): FTIR spectrum of *Aerva lanata* leaf extract

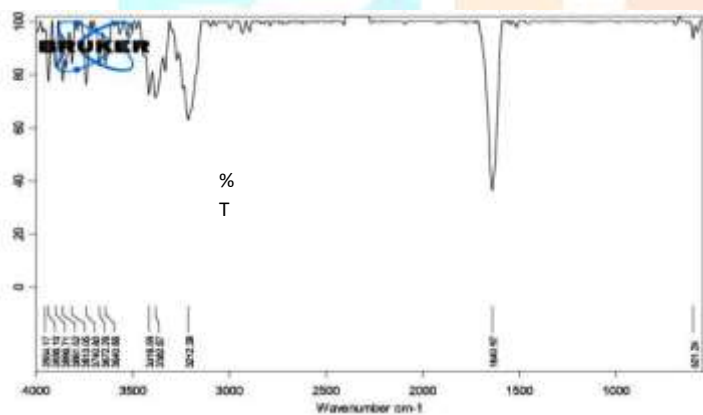


Figure 3(b). FTIR spectrum of Ag-Ni BMNPs in leaf extract

The strong intense peaks between  $3200\text{ cm}^{-1}$  to  $3950\text{ cm}^{-1}$  may be due to N-H, O-H stretching of  $1^{\circ}$  amines and polyhydroxy groups present in the extract. The strong absorption at  $1643\text{ cm}^{-1}$  indicates the presence of C=O group of amides. This result gives us the evidence about the high protein content of the extract. The small peak at  $2892\text{ cm}^{-1}$  may be due to C-H symmetrical stretching of methylene groups. The peak position at  $1519\text{ cm}^{-1}$  may be due to C=C stretch of aromatic ring. The peak at  $598\text{ cm}^{-1}$  is denoting the presence of C-Cl group.

The FTIR spectrum of Ag-Ni BMNPs exhibits major peak positions at  $3212\text{ cm}^{-1}$ ,  $3416\text{ cm}^{-1}$  and  $3382\text{ cm}^{-1}$  which indicate the N-H stretching vibrations of amines and O-H stretching of hydroxyl groups of alcohols and phenols. Intense peak at  $1640\text{ cm}^{-1}$  is due to C=O stretching of amide group. Very small peak at  $602\text{ cm}^{-1}$  indicates the presence of C-Cl group.

FTIR analysis clearly confirms that all the aforementioned absorption peaks of the extract are barely shifted in the FTIR spectrum of Ag-Ni BMNPs as the phyto molecules of the extract act as bioreducing agents, capping and stabilizing agents for the synthesized nanoparticles. The existence of these IR bands also in the Ag-Ni BMNPs confirmed that the surface of the nanoparticles was covered by plant secondary metabolites such as carbohydrates, glycosides, Saponin, phytosterols, phenolic compounds, tannins, flavonoids, proteins, aminoacids, diterpenes, carboxylic acids, amides, ketones, alkyl halides. [18]



### 3.3.SEM and EDX analysis:

From energy dispersive X-ray analysis we can analyze all the elements present in the BMNPs prepared by *Aerva lanata* leaf extract. **Figure.4** and **Table.1** show EDX spectrum and elemental composition respectively. This indicates the presences of Ag and Ni which confirms the formation of Ag-Ni bimetallic nanoparticles. This is also supported by the EDX study which gives quantitative data of silver and nickel compositions in BMNPs . Scanning electron microscopic (SEM) images of Ag-Ni BMNPs with various magnifications are given in **Figure 5**. From this it can be clearly noted that the prepared Ag-Ni bimetallic nanoparticles are in the size range between 50 and 100 nm in diameter.

**Table: 1.** Quantitative results of Ag-Ni BMNPs

Element	Weight %	Atomic %
Ni L	16.17	16.95
Ag L	73.06	41.67
O K	10.76	41.38
Totals	100.0	100.0

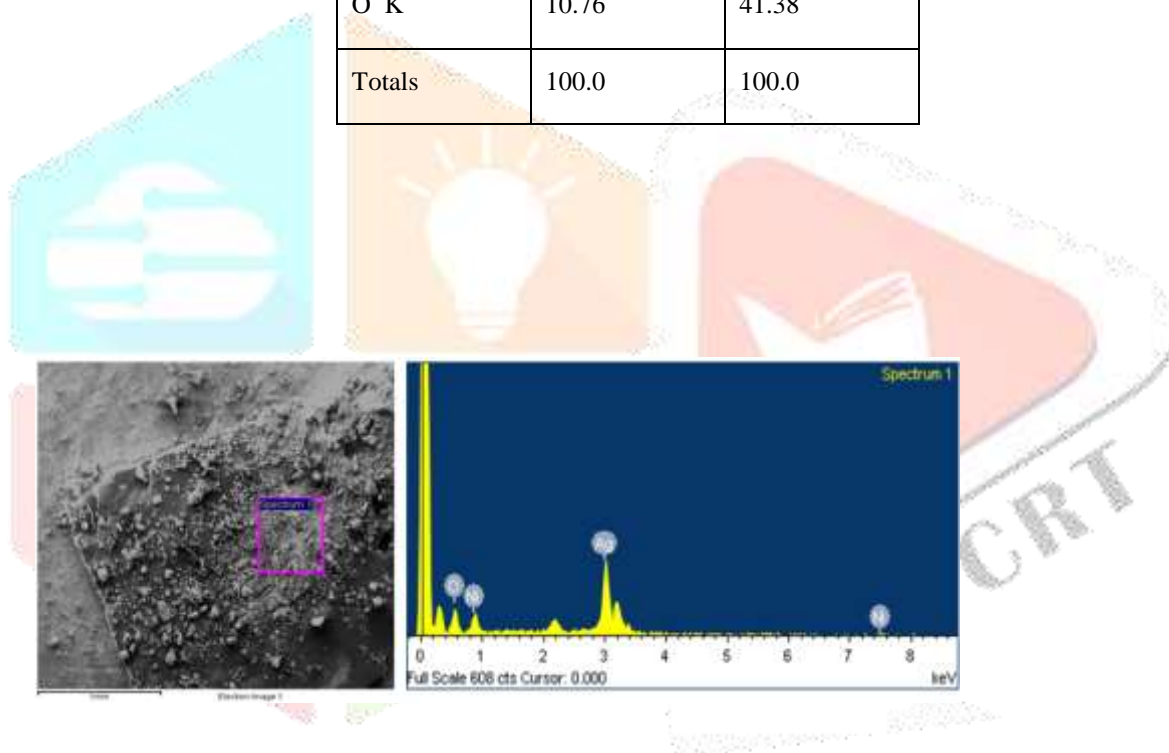


**Figure 4 :** EDX Analysis of Ag-Ni BMNPs

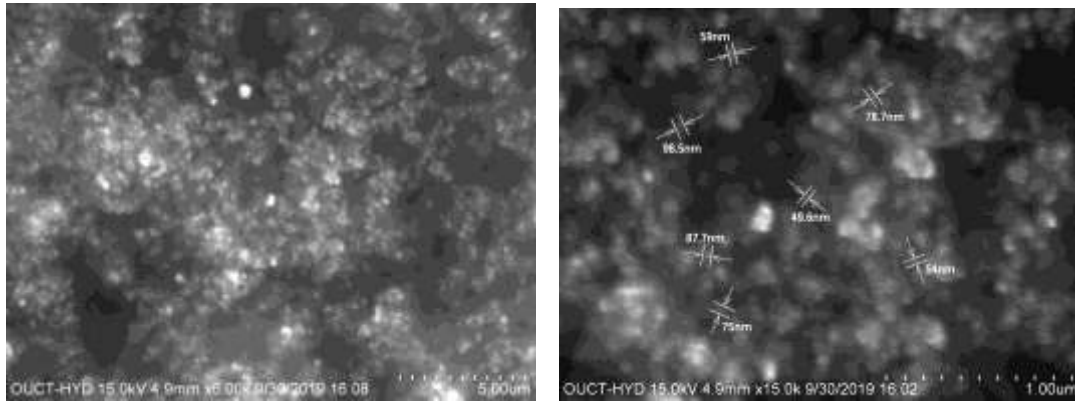


**Figure.5** : SEM images of Ag-Ni BMNPs

3.4. **HRTEM analysis:** **Figure.6** shows the high resolution transmission electron microscopy (HRTEM) images for synthesized Ag-Ni BMNPs from *Areva lanata* leaf extract. From these images, it was observed that Ag-Ni BMNPs were formed with spherical morphology and crystalline structure below 100 nm in size. More specifically, the two metal nanospheres appear to be positioned adjacent to each other. It is also in strong accordance with the images from SEM analysis.

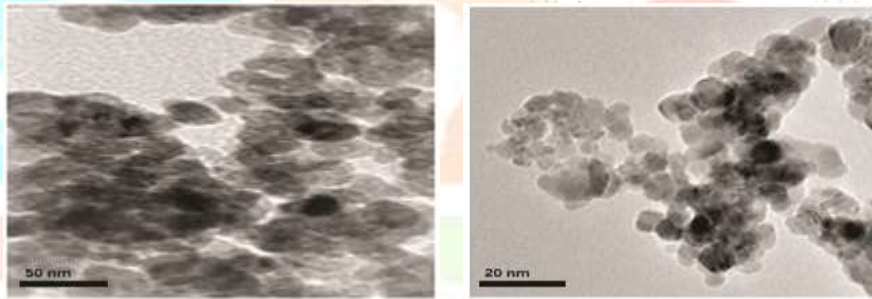


**Figure .6** : HRTEM images of Ag-Ni BMNPs

3.5. XRD analysis :

The XRD spectrum of green synthesized Ag-Ni BMNPs from leaf extract is shown in **figure: 7**.

The peaks appeared at  $2\theta$  values of  $38.20^\circ$ ,  $44.36^\circ$ ,  $64.40^\circ$ ,  $77.42^\circ$  correspond to the Bragg's reflections of Ag(111), Ag(200), Ni(111), Ag(220), Ni(222), Ag(311) planes respectively of face centered cubic crystal structure [19] as shown in the **Figure:7**

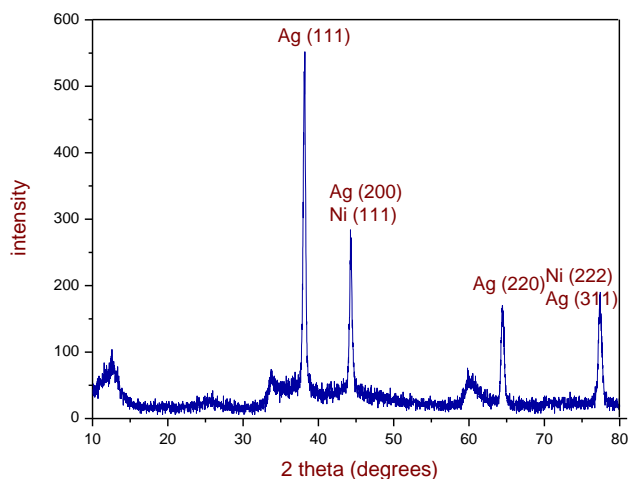


**Figure:7 .** XRD spectrum of Ag-Ni BMNPs

The average size D (in nm) of Ag-Ni bimetallic nanoparticles was calculated by using Debye-Scherrer equation (1).

$$D = \frac{K\lambda}{\beta \cos\theta} \dots\dots\dots(1)$$

D = crystalline size of Ag-Ni BMNPs

$\lambda$  = wavelength of x-ray source (0.15406 nm) used in XRD

$\beta$  = full width at half maximum (FWHM) of the diffraction peak

K = Scherrer constant = 0.9

$\theta$  = Bragg's angle

S.no.	2 $\theta$ (degrees)	$\theta$ (radians)	Cos $\theta$	$\beta$ (radians)	D (nm)
1	38.20 <sup>0</sup>	0.3333	0.9450	0.00714	20.5495
2	44.36 <sup>0</sup>	0.3871	0.9260	0.00664	22.5503
3	64.40 <sup>0</sup>	0.5620	0.8462	0.00686	23.8855
4	77.42 <sup>0</sup>	0.6756	0.7803	0.00673	26.4031



The numerically calculated value of the synthesized Ag-Ni BMNPs materials corresponds to an average particle size of **23.3471 nm**.

#### 4. Photodegradation studies on Malachite Green dye using Ag-Ni BMNPs :

The photo degradation experiments are carried on Malachite Green dye using green synthesized Ag-Ni BMNPs acting as a catalyst. Initially, 50 ppm of malachite green stock solution was prepared. Then reaction mixtures were prepared by adding certain amount of Ag-Ni BMNPs ( 10 mg, 20 mg, 30 mg, 40 mg, 50 mg, 60 mg,70 mg,80 mg ) to 100 mL of malachite green for distinct concentrations( 5 ppm, 10 ppm, 15 ppm, 20 ppm, 25 ppm, 30 ppm, 35 ppm). The pH of the reaction mixtures was maintained in the experiments at various values for both acidic and basic range ( i.e. pH 3,4,5,6,7,8,9,10,11 ) by adding 0.1 N H<sub>2</sub>SO<sub>4</sub> or 0.1 N NaOH solutions when required. Now this mixture was agitated for 20 minutes in dark condition to attain adsorption-desorption equilibrium between malachite green and Ag-Ni BMNPs. Sun light was used as irradiating source to reaction mixture for studying photodegradation during 11.00 am to 3.00 pm. At regular 30 minutes time intervals, aliquot part of the reaction mixture was taken, centrifuged to remove the photocatalyst particles and optical absorption properties were analyzed by using UV-Visible Spectrophotometer . The absorbance was observed by varying parameters like changing the time of contact between the catalyst and the dye, pH of the reaction mixture, concentration of the dye solution, dosage of the catalyst. Malachite green shows the highest absorption at 617 nm. [20].To determine the percentage degradation of MG dye solution following equation (2) was used.

$$\% \text{ degradation} = \left( \frac{A_0 - A_t}{A_0} \right) \times 100 \dots (2)$$

Where,  $A_0$  is the initial absorbance of the MG solution at zero minutes and  $A_t$  is the absorbance of the degraded solution after time  $t$  minutes.

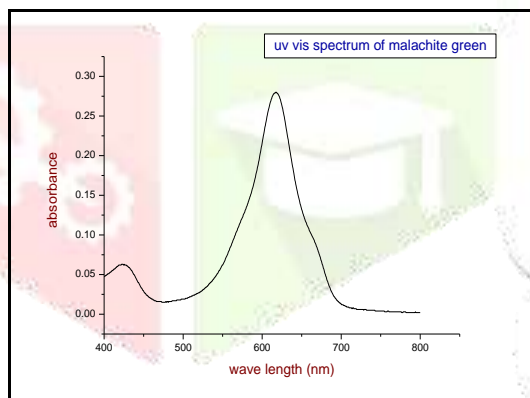
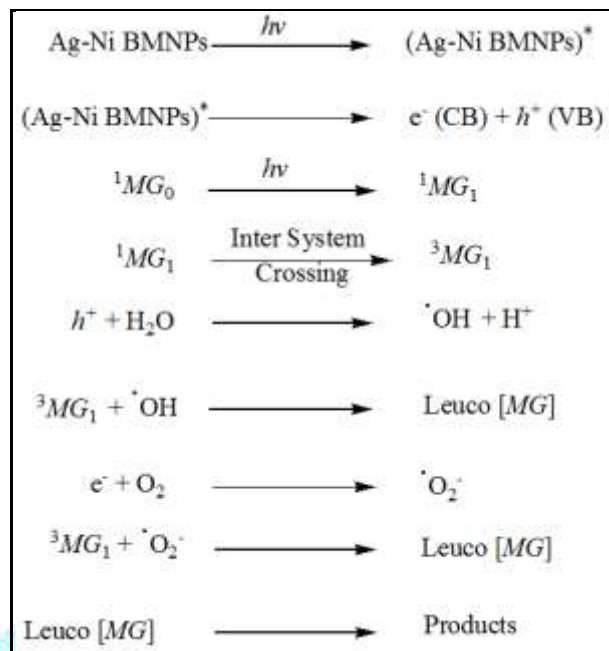


**Figure 8(a):** UV- VIS spectrum of Malachite Green

To study the photocatalytic activity of the Ag-Ni BMNPs on malachite green visible region of the light source was selected on UV-visible spectrophotometer . Absorption spectrum of 10 ppm malachite green solution was shown in **Figure 8(a)**. Highest absorption peak at 617 nm was observed and this maximum absorption peak was considered to monitor the photodegradation reaction of MG dye for all further studies in this paper.

## 4 (a) . Probable Mechanism of Photocatalytic degradation of MG dye with Ag-Ni BMNPs

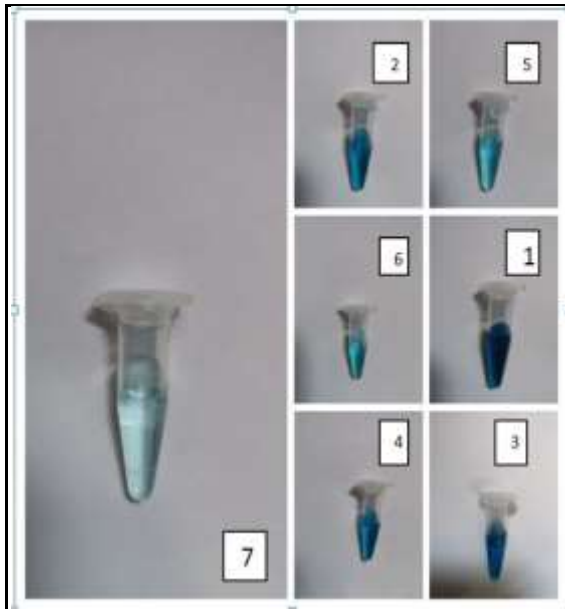


By absorbing suitable wavelength radiations MG dye goes to its first excited singlet state. Then by undergoing intersystem crossing (ISC) it enters into the triplet state. In the intervening time Ag-Ni BMNPs also absorb the radiant energy to excite its electron from valence band to the conduction band. The hole abstracts an electron from  $\text{H}_2\text{O}$  to generate  $\cdot\text{OH}$  radical and  $\text{H}^+$ .  $\cdot\text{OH}$  radical oxidizes the MG dye to its leuco form degrades into colourless product. The electron will be abstracted by oxygen molecule generating superoxide anion radical ( $\cdot\text{O}_2^-$ ). The formed anion radical reduce the MG dye to its leuco form, which on degradation forms products.

## 4.1. Effect of time of contact :

Photodegradation capacity of the Ag-Ni BMNPs on malachite green dye was studied in the presence of sunlight by batch mode experiments. The efficiency of BMNPs photocatalyst on degradation of MG is expected to be increased by increasing contact time. The effect of contact time was carried out by taking 10 ppm of 100 ml MG dye solution and 10 mg of BMNPs (pH at 7) as catalyst load which is shown in **Figure 8(b)** and **Figure 8 (c)**. From the initial part of the graph i.e upto 120 min, % photodegradation was exhibiting rapid rise. However, above 120 min the slope is relatively less steeper although % photodegradation remains still considerably predominant thus shows higher values.

Thus, upto 120 min, the % photodegradation of the dye by using the BMNPs photocatalyst was found to be rapid, and above 120 min it becomes relatively less rapid although active even upto 180 min. This is due to strong adsorption forces that predominate between the dye and the BMNPs as the number of the reactive sites on the photocatalyst were largely vacant during initial periods of contact time. But after 120 minutes of contact period, equilibrium between the number of vacant sites of adsorption and the dye molecules appears to be established although at slower rate, hence exhibit slightly slower rise of % photodegradation. [21]



(1) 0 mins (2) 30 mins (3) 60 mins (4) 90 mins  
(5) 120 mins (6) 150 mins (7) 180 mins

**Figure 8(b): Colour change in MG dye after addition of Ag-Ni BMNPs at various time intervals**

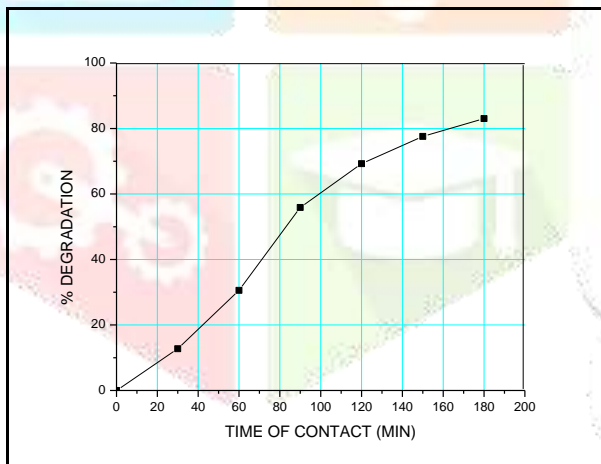


**Figure 8(c): Effect of contact time on photo degradation**

#### 4.2. Effect of initial concentration of MG dye solution :

Initial concentration of MG dye solution is also expected to effect the rate of photo degradation. To investigate this fact, dosage of BMNPs nano catalyst was kept constant at 10 mg , maintaining the dye solution pH at 7 and the time of irradiation as 180 minutes. However one parameter the initial concentration of the MG dye solutions was varied at 5 ppm, 10 ppm, 15 ppm, 20 ppm, 25 ppm , 30 ppm and 35 ppm. The rate of photodegradation can be represented graphically in **Figure 8(d)**.

It can be observed from the figure that the maximum photodegradation is found at 5 ppm, then it decreases with further rise in the concentration of MG dye solution. Thus as the initial concentration of the dye increases beyond 5 ppm, % photodegradation decreases[22]. This observation can be explained by the fact that at the low initial concentration of the dye solution, large number of dye molecules could be adsorbed on the surface of BMNPs . Increasing the initial concentration of the dye can result competitive adsorption among the dye molecules while the area of active reaction sites on the catalyst is fixed. Consequently the % photodegradation of MG dye decreases.

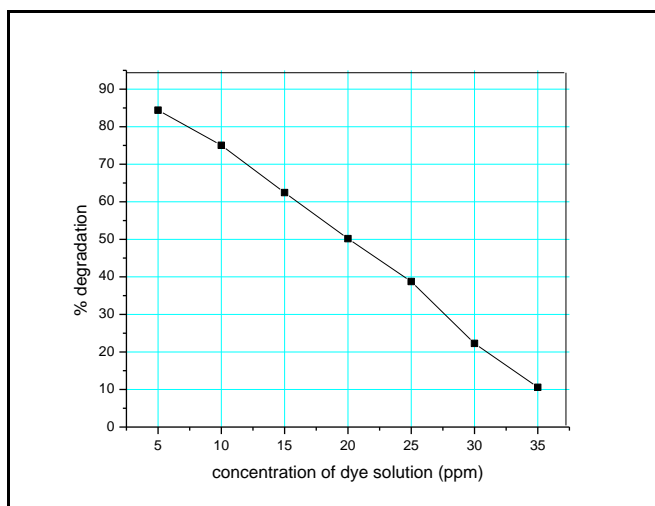


**Figure.8(d):** Effect of concentration of MG dye solution on photodegradation

### 4.3. Effect of pH:

pH of dye solution can influence the adsorption of dye on the photocatalyst. Keeping pH as variable, all other parameters were kept constant viz. the initial concentration of the malachite green solution was taken as 10 ppm, the concentrations of the photocatalyst as 10 mg and with time of irradiation 120 minutes. Different solutions of various pH values from 3 to 11 were prepared. Photodegradation efficiencies were compared which was shown in **Figure: 8(e)**.

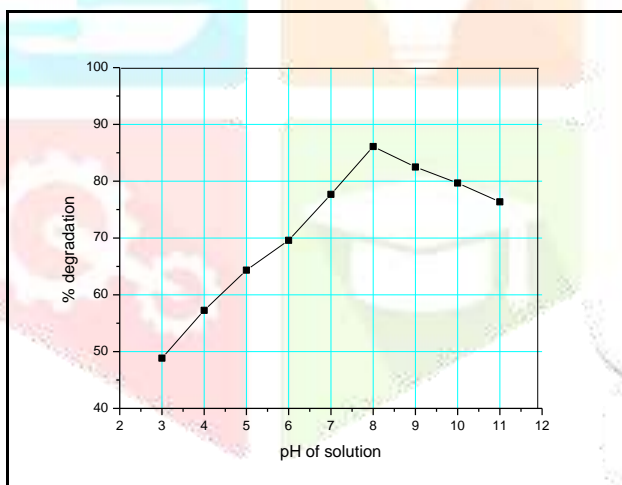


**Figure:8(e):** Effect of pH on photo degradation

It is observed that by increasing pH of the MG dye solution, the % photodegradation of MG dye on the photocatalyst enhances up to pH 8 and on further increase of pH, the rate of photodegradation was diminished. At pH less than 4 lower values of % photodegradation of the dye by the catalyst was observed. Solution pH may influence both solution chemistry and surface active sites of the adsorbent. At acidic pH,  $H^+$  ions of the water molecules, may race with dye ions for the adsorption sites of the catalyst surface, there by hindering the adsorption of the dye. As the pH value increases, the number of  $H^+$  ions of the aqueous solution reduces, hence the cationic dye molecules could approach the catalyst surface at a faster rate, thus exhibit an fast increase in the rate of % photodegradation. At pH 8 the adsorption is maximum, hence the photo degradation was found to be maximum. At pH >8, the malachite green dye may not be maintained in its cationic form due to high concentration of  $OH^-$  ions in the aqueous dye solution. Consequently, the electrostatic repulsion increases between the MG dye and negatively charged catalyst surface. As a result the photodegradation slowly decreases from pH 8 to 11. [23]

#### 4.4. Effect of dosage of photo catalyst:

In photodegradation process, one of the important parameters of decolourizing of dye solution is dosage of the photocatalyst. To avoid splurge of costly catalyst and attain the maximum absorption of photons optimization of the catalyst dosage is important. For this, dosage amount was varied from 10 mg to 80 mg taken in 100 ml of 10 ppm MG dye at pH 8 with contact time 120 minutes. The degradation of MG was shown in figure 8(f).

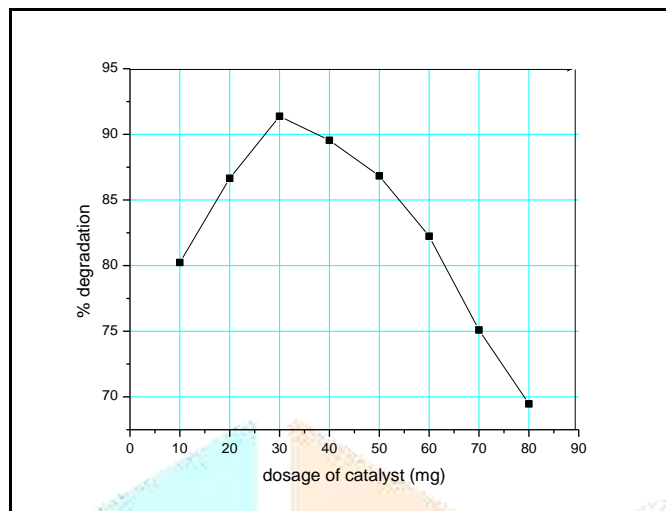


Figure 8(f): Effect of dosage of catalyst on photo degradation

From the graph it can be concluded that, by increasing dosage of catalyst from 10 mg to 80 mg in 100 ml dye solution, the % photodegradation of the MG dye shows an increasing trend upto 30 mg. This is because the increase in amount of catalyst upto 30 mg would increase the number of reactive sites that produce more reactive species [24]. On further increase of catalyst dosage, % photodegradation of MG dye decreases because the catalyst particles form more turbid suspensions at higher loadings, which increase the scattering of the solar light and reduce the penetration of light into the reaction mixture.

#### CONCLUSION

An ecologically safe method is projected in this report to synthesize Ag-Ni bimetallic nanoparticles from *Areva lanata* leaf extract. From UV-VIS spectral analysis it is confirmed that the particles are in nanoscale as per the positions of the Surface Plasmon Resonance (SPR) bands. FTIR data confirms the presence of secondary metabolites of phyto molecules that act as the bio reducing and capping agents of the formed nanoparticles. Results of XRD, SEM and TEM analyses proved that Ag-Ni BMNPs are in spherical morphology and cubic crystalline structure with size between 20-100 nm. The photocatalytic activity of these nanoparticles is examined under sunlight for degradation of MG dye which is an environmental pollutant. The % photodegradation of MG dye changes with parameters such as contact time, concentration of MG dye, pH, photocatalyst dosage. From this research study on bimetallic Ag-Ni BMNPs synthesized from *Areva lanata* leaf extract, the optimum conditions found in the degradation of MG dye is pH 8, weight of catalyst 30 mg, dye concentration of 10 ppm and contact time of 120 minutes. A maximum photodegradation of ~ 85-89% could be obtained under these optimum conditions.

#### ACKNOWLEDGEMENT

Authors are thankful to Department of Engineering Chemistry, A.U College of Engineering (A), Andhra University for providing general lab facilities for the entire bench work.



## REFERENCES

1. The Nanotechnology Toolkit. (2010). *Introduction to Nanoscience and Nanotechnology*, 96–175
2. Venkatesan, P., & Santhanalakshmi, J. (2012). Core-Shell Bimetallic Au-Pd Nanoparticles: Synthesis, Structure, Optical and Catalytic Properties. *Nanoscience and Nanotechnology*, 1(2), 43–47
3. Srinoi, P., Chen, Y.-T., Vittur, V., Marquez, M. D., & Lee, T. R. (2018). Bimetallic Nanoparticles: Enhanced Magnetic and Optical Properties for Emerging Biological Applications.
4. Singh, P. K., & Kundu, S. (2019). Rapid green synthesis of noble Bimetallic nanoparticles
5. Saito, G., Nakasugi, Y., Yamashita, T., & Akiyama, T. (2014). Solution plasma synthesis of bimetallic nanoparticles. *Nanotechnology*, 25(13), 135603
6. Singh, P. K., & Kundu, S. (2019). Rapid green synthesis of noble Bimetallic nanoparticles
7. S.M.Roopan, T. V. Surendra, G.Elango and S. H. S. Kumar, *Applied Microbiology and Biotechnology*, 2014, 98(12), 5289–5300
8. Murmat., S. (2017). Optimization Of Azo-Dyes To Reduce Environmental Impact Of Textile Industries. *International Journal of Advanced Research*, 5(11), 1519–1528
9. Hidayah, A. N., Faridah, S., Azura, M. N., Gayah, A., Othman, M., & Fatimah, A. (2016). Malachite Green and Leuco-Malachite Green Detection in Fish Using Modified Enzyme Biosensor. *Procedia Chemistry*, 20, 85–89
10. Srivastava, S., Sinha, R., & Roy, D. (2004). Toxicological effects of malachite green. *Aquatic Toxicology*, 66(3), 319–329.
11. Doble, M., & Kumar, A. (2005). Degradation of Dyes. *Biotreatment of Industrial Effluents*, 111–122.
12. Chen, F., He, J., Zhao, J., & Yu, J. C. (2002, February 19). Photo-Fenton degradation of malachite green catalyzed by aromatic compounds under visible light irradiation.
13. Helaili, N., Boudjamaa, A., Kebir, M., & Bachari, K. (2017). Efficient photo-catalytic degradation of malachite green using nickel tungstate material as photo-catalyst. *Environmental Science and Pollution Research*, 24(7), 6481–6491
14. Kang, S.-F., Liao, C.-H., & Po, S.-T. (2000). Decolorization of textile wastewater by photo-fenton oxidation technology. *Chemosphere*, 41(8), 1287–1294
15. Zheng, X., & Lombardi, J. R. (2008). Light-induced growth of monodisperse silver nanoparticles with tunable SPR properties and wavelength self-limiting effect. *Plasmonics: Metallic Nanostructures and Their Optical Properties VI*.
16. Mallabaev, A., Rakhimov, D. A., & Murdakhaev, Y. M. (1989). Carbohydrates of *Aerva lanata*. *Chemistry of Natural Compounds*, 25(3), 369–370.
17. Zapesochnaya, G. G., Kurkin, V. A., Okhanov, V. V., Perzykh, L. N., & Miroshnikov, A. I. (1991). Structure of the alkaloids of *Aerva lanata*. *Chemistry of Natural Compounds*, 27(6), 725–728.
18. Baltaev, U. A., Murdakhaev, Y. M., & Abubakirov, N. K. (1992). Phytoecdysteroids of *Aerva lanata*. *Chemistry of Natural Compounds*, 28(1), 123–124
19. Sridharan, K., Endo, T., Cho, S.-G., Kim, J., Park, T. J., & Philip, R. (2013). Single step synthesis and optical limiting properties of Ni–Ag and Fe–Ag bimetallic nanoparticles. *Optical Materials*, 35(5), 860–867.
20. Liang, S., Jia, Z., Zhang, W., Wang, W., & Zhang, L. (2017). Rapid malachite green degradation using Fe<sub>73</sub>Si<sub>13</sub>B<sub>9</sub>Cu<sub>1</sub>Nb<sub>3</sub> metallic glass for activation of persulfate under UV–Vis light. *Materials & Design*, 119, 244–253.
21. Weng, X., Huang, L., Chen, Z., Megharaj, M., & Naidu, R. (2013). Synthesis of iron-based nanoparticles by green tea extract and their degradation of malachite. *Industrial Crops and Products*, 51, 342–347.
22. Modirshahla, N., Behnajady, M. (2006). Photooxidative degradation of Malachite Green by UV/H<sub>2</sub>O<sub>2</sub>: Influence of operational parameters and kinetic modeling. *Dyes and Pigments*, 70(1), 54–59.
23. Pandian, A. M. K., Karthikeyan, C., & Rajasimman, M. (2017). Isotherm and kinetic studies on adsorption of malachite green using chemically synthesized silver nanoparticles. *Nanotechnology for Environmental Engineering*, 2(1).
24. Batool, M. (2018). Degradation of Malachite Green by Green Synthesized Copper Nanoparticles by Using Aloe Barbadensis Leaf Extracts. *Archives of Nanomedicine: Open Access Journal*, 1(2).